Multi-objective optimization of helium power cycle for thermo-chemical energy storage in concentrated solar power

Energy Conversion and Management: X 12 (2021) 100116

Contents lists available at ScienceDirect

Energy Conversion and Management: X

journal homepage: www.sciencedirect.com/journal/energy-conversion-and-management-x

Multi-objective optimization of helium power cycle for thermo-chemical energy storage in concentrated solar power

Umberto Tesio *, Elisa Guelpa, Vittorio Verda

Energy Department, Politecnico di Torino, Turin, Italy

ARTICLE INFO

Keywords:
Calcium-looping
Long-term energy storage
Indirect integration
Brayton cycles
100% renewable

ABSTRACT

Concentrated Solar Power is an increasingly widespread technology because of its potential for efficiently converting solar radiation into electricity. The discrepancy between the time evolution of solar radiation and power demand makes it appropriate to include a Thermal Energy Storage in the plant operation. Calcium-Looping represents an interesting opportunity to store solar energy in chemical form thanks to high energy density and null thermal losses. Several aspects must be taken into account for the choice of the thermal cycle in the discharging process and its optimization. Process components operating conditions, heat transfer processes, layout complexity and investment costs are the most important characteristics for which an appropriate investigation must be developed. In this context, thanks to the high achievable temperatures and efficiencies, the use of helium power cycles constitutes an attractive option to analyse. The present work is devoted to the study of this thermal cycle integration and its optimization in energy and economic terms; a multi-objective optimization is performed with the aim of evaluating possible compromises between these two aspects. The system synthesis, design and operating conditions are optimized thanks to the adoption of a coherent and comprehensive strategy, which is the HEATSEP method. To evaluate the effect of deviations in the estimation of helium turbomachinery price, a sensitivity analysis is performed, showing that the plant configurations obtained do not change even for considerable errors in the prediction of this cost. He turbine inlet temperature and minimum temperature difference of He regenerator are demonstrated to strongly impact the cost of the system. Results show total plant efficiencies in a range between 18.1% and 21.9% and novel system layouts are designed for the most significant configurations. The strategy for the power block thermal feeding appears to be a key element in both energy and economic terms.

1. Introduction

During the last years, Concentrated Solar Power (CSP) played an important role among the renewable energy sources and very promising outlooks are predicted for its future [1]. The possibility to store thermal energy makes it an interesting option in the perspective of clean and dispatchable generation of electricity [2]. Operating temperatures, thermal losses, process efficiency and energy density are the most important aspects to properly select Thermal Energy Storages (TES) for CSP applications [3]. Despite Parabolic Through Collectors with TES based on molten salts represent the most widespread technology at commercial level [4], Thermo-Chemical Energy Storage (TCES) for central tower plants aroused recently a great interest because of their various potentials [5]. Between the known alternatives, the reversible reaction exploited in Calcium-Looping (CaL) is recognized as one of the options that is mostly worth to investigate [6]. The charging process relies on the calcination endothermic reaction and is performed in a chemical reactor named calciner. The calcium carbonate is transformed into calcium oxide and carbon dioxide by the thermal energy provided by solar radiation. The reversed process (carbonation) occurs during the discharging phase in the carbonator (Eq. (1)).

$$CaCO_{3(s)} + HEAT \leftrightarrow CaO_{(s)} + CO_{2(g)} \quad \Delta H_r^0 = \pm 178 \frac{kJ}{mol} \tag{1}$$

It is important to take into account the non-idealities affecting the Calcium-Looping process since the reaction is not perfectly reversible [7]. Consequently, only a fraction of CaO provided to the carbonation participates actively to the reaction, while the remaining part acts as inert matter and is still present in the reactor outflows. The mechanisms at the base of this aspect are deeply investigated in [8–10]. The parameters that are found to mostly influence this phenomenon are dimensions and porosity of solid grains, as well as calcination temperature

* Corresponding author.

https://doi.org/10.1016/j.ecmx.2021.100116
Received 15 July 2021; Received in revised form 7 October 2021; Accepted 9 October 2021
Available online 23 October 2021

[11]. CaO conversion (X) is the parameter used to describe CaO deactivation and is defined as the ratio between the calcium oxide that reacts with the carbon dioxide and the total amount provided to the reactor.

There are two ways to integrate a TCES based on CaL in a CSP plant: directly or indirectly. It is worth to notice that the differences between these alternatives are only related to the discharging phase. In the first case, the power production is realized with a closed Brayton cycle in which the CO_2 stream exiting the carbonator is expanded, cooled down, compressed and recirculated in the process. In the second case, a separate Power Block (PB) is thermally fed through a heat exchange performed on the sensible heat contained in the carbonator outflows. Consequently, it is possible to employ a great variety of fluids and thermal cycles. In this case the achievable pressures are not constrained by the carbonator operating conditions. The most suitable alternatives are represented by high temperature Organic Rankine cycles [12], Steam Rankine cycles [13] and Brayton-Joule cycles [14]. In case of sensible energy storage, the most common methods employed for the plant optimization are the heuristic methods, since they are able to manage nonconvex and discontinuous functions. The Genetic Algorithm (GA) is used in [15–17], but Particles Swarm Optimization (PSO) is a suitable choice as well [18,19]. However, if the number of variables is relatively high ($\geq 10^3$), deterministic algorithms are preferred [20,21], despite they may require a more complex implementation in order to delete or properly manage the sources of non-convexity.

The direct integration is deeply analyzed in [22] and [23], where the plant layout is designed through pinch analysis [24] and the optimal operating conditions are found with a sensitivity analysis in order to maximize the system efficiency. The possibility to store the solid reactants at high temperature is evaluated in [25], while a comparison between direct and indirect integrations is performed in [26]. A comprehensive review of Calcium-Looping process for CSP is reported in [27]; the state of the art of this technology and the results of the researches already made provide useful information for the understanding of both advantages and issues to be solved characterizing this kind of system.

Considering the analyses found in literature, it is possible to identify the research gaps and draw some conclusions: 1) CaL indirect integration represents a field in which are still needed deeper investigations, especially innovative Brayton cycles integrations; 2) sensitivity analysis is often employed in literature but its extent in terms of optimization is limited; 3) power cycles operating conditions and thermal transfer processes are both fundamental aspects to optimize in order to achieve high efficiencies; 4) technical constraints due to the early stage of development of CaO technology must be taken into account to perform a coherent study; 5) Cal integrations have been mainly investigated excluding the plant section corresponding to the Solar Side, but this part should be considered since it has an important impact on the performances and capital costs.

The present work can be seen as an expansion of the previous studies reported in [28] and [29]. The novelty of this paper consists in analyzing in both energy and economic terms the indirect integration of a helium power cycle in a Central Tower CSP plant with TCES based on CaL. This is a configuration that has not yet been investigated; the plant layouts obtained and the resulting performances are therefore completely new. All the treated aspects are considered and analyzed with a multi-objective optimization. For this purpose, a comprehensive methodology for the optimization of operating conditions and heat transfer processes is adopted, able to manage the choice of the power block configuration among various alternatives. This aspect represents an important difference compared to the other works in the scientific literature, where the synthesis and design problems are not addressed or are only treated with a sensitivity analysis. Performances, costs and layouts simplicity are the parameters considered for the estimation of the bast design of the plant.

2. Case study

The case study investigated in the present work is represented in simplified form in Fig. 1. The charging process takes place in the calciner side, which is the plant section between the receiver and the storages. Here, the $CaCO_3$ is preheated and sent to the solar receiver, where through the calcination is converted into CaO and CO_2; these two products are cooled down and stored in their respective vessels. Being in gaseous state, it is necessary to compress (Storage Compressor, ST) the carbon dioxide from 1 bar up to 75 bar in order to achieve reasonable storage volumes [22]. For this purpose, intercooled compression is a suitable choice to decrease the energy consumption. The discharging phase occurs in the system portion between the storages and the thermal cycle. The two reactants are preheated and, once the CO_2 is expanded (Storage Turbine, ST) to reach the carbonator operating pressure, they enter the reactor. In the exit section, both the carbonator outflows are cooled down and the $CaCO_3$ (with the unreacted CaO) is sent to its storage while the CO_2 in excess pass through a Blower (B) and is recirculated in the process.

In order to perform an analysis as comprehensive as possible, two alternatives are taken into account to provide heat to the power block. In the first case, a Heat Recovery is performed on the Carbonation Products (HRCP, A in Fig. 1), while in the second case a Heat Transfer is executed on the Carbonator Wall (HTCW, B in Fig. 1). An Entrained Flow reactor is assumed for HRCP, while Fluidized Bed carbonator is chosen in case of HTCW.

Finally, it is important to observe that the configuration analyzed do not exploit external heating sources in order to achieve 100% renewable operating conditions.

3. Plant simulation and optimization model

The following subparagraphs are devoted to the explanation of the simulation and optimization strategies adopted for the corresponding plant sections. As simplifying hypothesis, the discharging process is assumed as stationary, while the dimensioning of the calciner side components is executed taking into account the time dependence due to the solar radiation. The entire optimization structure is schematized in Fig. 2; terms in orange represent the optimizations of operating conditions (temperatures, pressures, flowrates, etc.) and terms in blue stands for optimizations of thermal transfer processes. The charging process is separately optimized with different strategies: pinch analysis for the heat transfer processes; sensitivity analysis for the Heat Exchanger Network dimensioning; and unconstrained NLP for the sizing of the heliostat field and solar receiver. Results of these optimizations are collected and used as inputs for the optimization of the discharging process (and therefore of the entire plant), which is performed with a Genetic Algorithm (for the synthesis, design, operating pressures and temperatures) in which are nested a bisection method (for finding the CaO flowrate) and the pinch analysis (again for the heat transfer processes). For a more detailed discussion of the method adopted make reference to [30] and [29]. The optimization strategy employed is structured such that the algorithm chooses the optimal power block layout and plant operating conditions according to the selected criteria.

3.1. Power block – Brayton cycle

Closed Brayton thermal cycles with helium as power fluid are an interesting alternative between the available options because of the expected high efficiencies [31] attainable tanks to the high operating temperatures and the thermophysical properties. The great majority of the studies that can be found in scientific literature on helium Brayton cycles are conducted in the field of nuclear power plants [32,33] but, in more recent works, these thermal cycles are also investigated for CSP [34,35]. Advantages and drawbacks characterizing He power blocks are highlighted in [36]: low (but non-negligible) pressure losses, good heat

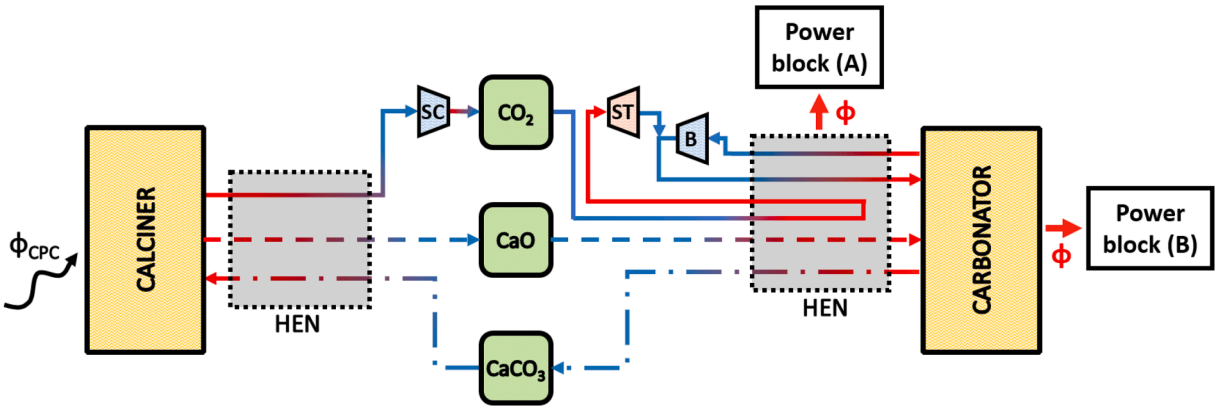

Fig. 1. Plant layout for the CaL indirect integration in a CSP plant.

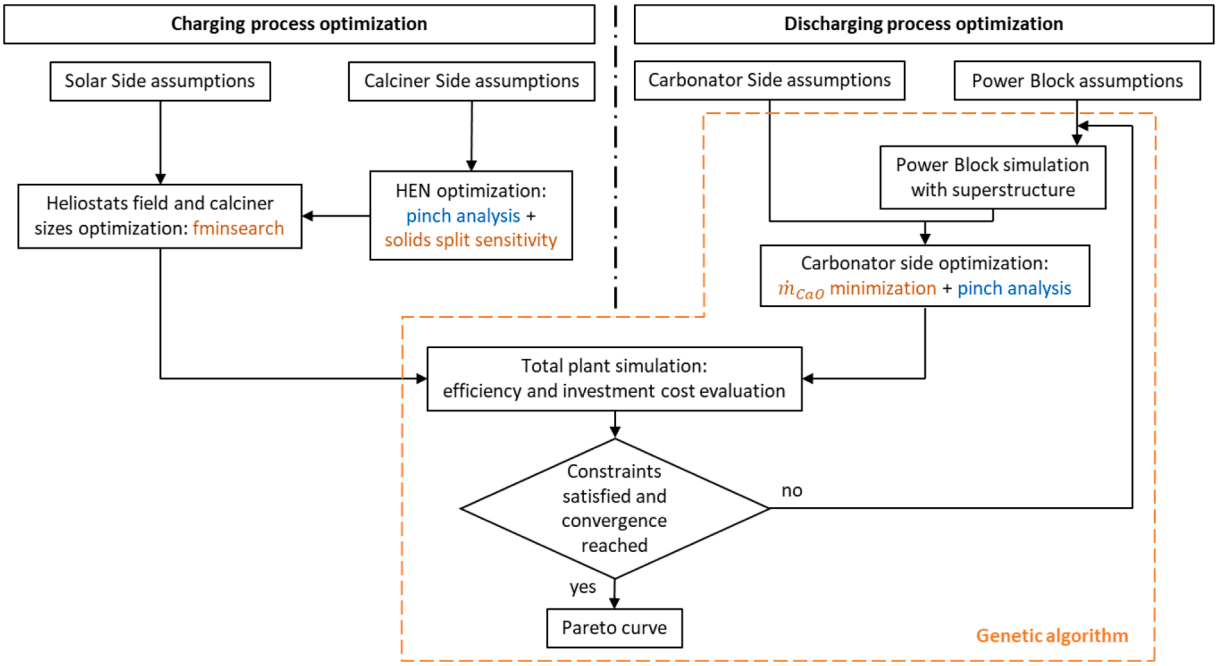

Fig. 2. Schematic of the complete optimization process.

transfer coefficients, no Mach number restriction, high number of turbomachinery stages, leakages and early stage of development. In addition, a comparison between helium and supercritical carbon dioxide cycles is performed in [37]. Some of the (already cited) aspects that characterize this technology must be carefully treated, since they have important effects either on the efficiency or on the investment costs. In particular: 1) high number of stages for turbomachinery (especially for compressors); 2) non-negligible impact of pressure drops in heat exchangers on cycle performance; 3) intercoolings/reheatings effects on efficiency.

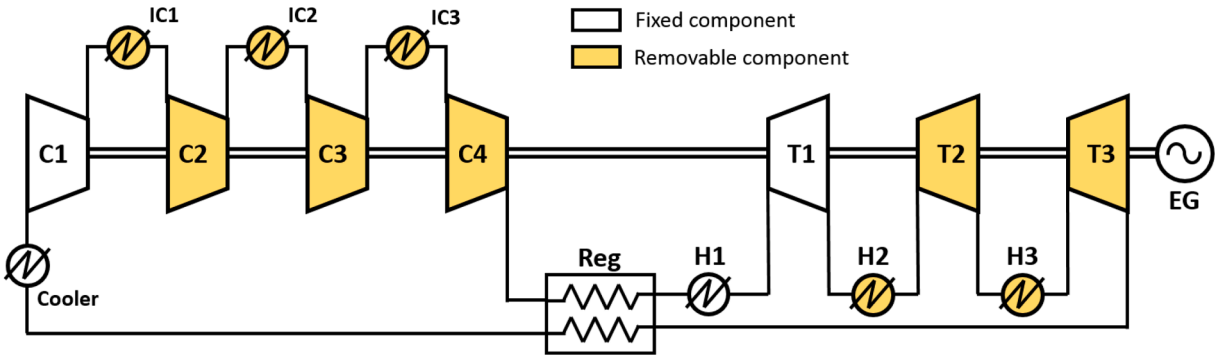

Fig. 3. He thermal cycle superstructure.

Concerning this last point, the number of intercoolings and reheatings are included between the independent variables of the problem through a superstructure. Up to four turbines and eight compressors are considered in the investigation executed in [38] but, in order to avoid an excessive layout complexity, three turbines and four compressors are set as maximum achievable number of turbomachinery. The total layout assumed for the optimization process is shown in Fig. 3.

In Table 1 are summed up the assumptions for the power block simulation; those are assumed as described in [35] and [39]. Helium is considered as ideal gas and dry cooling with ambient air is adopted in the coolers.

Pressure losses occurring in the regenerator are set as a function of the Mean Logarithmic Temperature Difference in order to take into account the fluidynamic drawbacks related to a more efficient regeneration. Constraints imposed to the power block are: 1) maximum turbine inlet pressure set to 75 bar; 2) equal turbines inlet temperatures; 3) net electrical power generation of 2 MW.

The independent variables to optimize are: first compressor inlet pressure (C1IP), number of compressors (#C), compressors pressure ratio (β_C), regenerator minimum temperature difference ($\Delta T_{min,reg}$), turbines inlet temperature (TIT), number of turbines (#T) and turbines pressure ratio (β_T). Those are reported in Table 2 with their respective variation ranges (assumed coherently with [35,40]).

3.2. Carbonator side and storages

The carbonator side optimization has to be carefully developed. In fact, operating conditions of process components, Heat Exchanger Network layout and thermal feeding of the power block have to be found taking into account their mutual influences. For this scenario, the HEATSEP method [41] is particularly suitable since it allows to deal with all the cited aspects. Very briefly, this methodology relies on the contemporary optimization of process components operation and heat transfer processes. The first one can be executed with an optimization algorithm, while the second (which is nested into the former one) can be solved using the pinch analysis. It is worth to notice that, using the pinch analysis, the carbonator side Heat Exchanger Network remains unknown during the optimization process and it can be designed only once that the optimization process is concluded. However, as later discussed, this does not represent a problem for the extent of the present work.

The chemical reactor is simulated with the same energy balance set in [22], while the Heat Exchanger Network is synthesized trying to avoid heat exchange between solids and splitting of solid streams [23]. Air cooling of solid streams is avoided with the aim of reducing the number of components in the Heat Exchanger Network.

Data assumed (according to [7,25;26]) for carbonator side operating conditions are summed up in Table 3.

Parameters taken as independent variables for the optimization of carbonator side are: CaO carbonator inlet temperature ($T_{CaO,IN}$), CO_2 carbonator inlet temperature ($T_{CO2,IN}$), carbonation temperature (T_{CARB}), blower inlet temperature (BIT), storage turbine inlet temperature (STIT) and CaO mass flowrate extracted from the storage ($\dot{m}_{CaO}$). Those are reported in Table 4 with their respective variation ranges (assumed coherently with [26]).

Table 1
Thermodynamic cycle parameters.

Parameter	Component/stream	Value
Polytropic efficiency	Turbine	$0.932–0.0117\cdot\ln(\beta_T)$
	Compressor	$0.916–0.0175\cdot\ln(\beta_C)$
Electrical efficiency	Electric generator	0.98
Pressure losses	Regenerator hot side	$19.2/\Delta T_{ml}$ %
	Regenerator cold side	$3.12/\Delta T_{ml}$ %
	Heater	2 %
	Cooler	1.6 %
Ambient temperature	Air	20 °C

Table 2
He cycle variables range.

Variable	Minimum	Maximum
C1IP	1.2 bar	26 bar
#C	1	4
β_C	1.16	5
$\Delta T_{min,R}$	5 °C	25 °C
TIT	600 °C	850 °C
#T	1	3
β_T	1.16	5

Table 3
Carbonator side assumptions.

Parameter	Component/stream	Value
Operation time	Carbonator side	24 h
CaO conversion	CaO	0.5
Thermal losses	Carbonator	1% of heat
Isentropic efficiency	Storage turbine	0.8
	Blower	0.8
Electrical efficiency	Electric generator	0.98
Pressure losses	Mixed CO2	6%
	Recirculated CO2	4%
	Storage CO2	1%
Storage temperature	Storage vessels	20 °C
CO2 storage pressure	CO2 vessel	75 bar
Solid conveying electrical consumption	CaO, CaCO3	10 kJ/(kg·100 m)
Storages-carbonator distance	CaO, CaCO3	100 m
Heat rejection electrical consumption	Coolers	0.8% of heat
Minimum ΔT	HEXs	15 °C

Table 4
Carbonator side variables range.

Variable	Minimum	Maximum
$T_{CaO,IN}$	310 °C	860 °C
$T_{CO2,IN}$	35 °C	860 °C
T_{CARB}	500 °C	875 °C
BIT	35 °C	400 °C
STIT	270 °C	650 °C
$\dot{m}_{CaO}$	–	

An additional constraint related to the thermal transfer process is added after a preliminary run. This is made in order to prevent the tendency shown by the algorithm in reaching a configuration in which is not possible to avoid solid–solid heat exchange in the carbonator side Heat Exchanger Network.

3.3. Calciner side

The calciner side optimization is performed by means of a simplified approach (0-Dimensional model of the reactor), taking into account the time-dependent behavior determined by the variation of solar radiation collected by the receiver. In other words, solar flux and mass flowrates passing through the reactor are not constant over the operating interval, but their variation is managed keeping their proportions, as simplifying assumption. Any other detail can be found in [28], where is developed a methodology for the simulation of the charging section that is adopted in the present study. Operating pressures and temperatures are assumed as constant in time during the charging phase. Parameters assumed for the operation of this plant section are reported in Table 5.

The Heat transfer is optimized through the pinch analysis. As a result, solid–solid thermal exchange cannot be avoided; this issue is overcome with the insertion of a heat transfer fluid between the two solid streams. In addition, the split ratio of $CaCO_3$ is optimized in order to minimize the Heat Exchanger Network investment cost.

The number of intercoolings in the compression of carbon dioxide is an independent variable, whose value is evaluate according to both

Table 5
Calciner side assumptions.

Parameter	Component/ stream	Value
Operating temperature	Calciner	950 °C
Cut-in power	Calciner	20% of calciner design power
Thermal efficiency	CPC	0.97
	Calciner	0.75
Isentropic efficiency	Compressors	0.8
Electrical efficiency	Electric motor	0.98
Pressure losses	CO_2 coolers	1%
Solid conveying electrical consumption	CaO, $CaCO_3$	10 kJ/(kg·100 m)
Storages-calciner distance	CaO, $CaCO_3$	100 m
Heat rejection electrical consumption	Coolers	0.8% of rejected heat
Minimum ΔT	HEXs	15 °C

energy and economic criteria.

3.4. Solar side

Similarly to the case of the calciner side, the Solar Side (SolS) is simulated with the methodology developed in [28]. The design day chosen for the plant is the winter solstice, considered as the most unfavorable day of the year. This guarantees that the daily power production is achieved for any other day of the year. Plant location, Direct Normal Irradiation and heliostat field efficiency are taken from [42]. With these inputs and the model of the plant sections under discussion (solar side and calciner side) taken from [28], it is possible to perform a 0-Dimensional simulation of the main components of the charging process, which is sufficient to obtain the information needed for the dimensioning and the estimation of the plant efficiency. The energy balance at the solar calciner is composed by: the solar radiation reflected by the heliostats entering the reactor; the thermal losses exiting the reactor; the solid $CaCO_3$ at the inlet; and the CaO and CO_2 at the outlet. With some calculation it is easy to observe that the heliostat field area and solar calciner size are the only two variables to determine in the equation. Therefore, these two parameters can assume multiple values that are equivalent in energy terms (since they satisfy the energy balance), but with a different impact in economic terms. For this reason, a suitable optimization is performed in order to design those components.

4. Economic analysis

For the economic analysis it is not necessary to perform a complete study on the whole plant lifetime or consider factors such as interest rates, since the consumption of any external energy source is excluded. In addition, since some costs (installation, contingencies, etc.) are calculated as a percentage of equipment costs, it is possible to perform an economic analysis estimating only the investment cost of components involved in the process. In other words, from the economic analysis of the present work it is not requested a detailed level of description, but only to provide an adequate benchmark for the comparison in financial terms of the feasible solutions of the optimization problem.

Relatively complex procedures and calculations are needed for the estimation of the investment costs; for this reason, in Table 6 are reported only the references of the cost functions chosen from the scientific literature. In alternative, the same cost functions are collected and actualized in [28].

In order to perform an analysis as consistent as possible, the following considerations are made:

- A suitable cost function for fluid–solid heat exchanger is developed according to [50];
- Investment cost of storages for solid reactants is assumed as negligible;
- Investment cost of fluidized Bed carbonator is estimated as indicated in [48] and an adequate correction (reported in Appendix A) is performed to take into account the different streams that exchange heat;
- Helium turbomachinery investment costs are estimated performing an equivalence with the case of turbogas technology (proposed in [51] for sCO_2 but also applicable to the present analysis with He) and the coefficients of the cost functions are adapted to the costs found in [52];
- A cost function is developed from preliminary simulations for the carbonator side Heat Exchanger Network;
- Global heat transfer coefficients (U, taken from [48;49]) for Heat Exchanger Networks dimensioning are reported in Table 7.

Table 6
References for estimation of components cost.

Component	Reference
Heliostat field	[43]
Central tower	[44]
Compound Parabolic Collector	[45]
Solar calciner	[45]
Carbonator (Entrained Flow)	[46]
CO_2 storage	[5,47]
Fluid-fluid Heat Exchanger	[48]
CO_2 blower	[48]
CO_2 compressor	[48]
CO_2 turbine	[48]
He regenerator	[49]
He cooler	[49]
Electric generator	[48]

5. Multi-objective optimization

The multi-objective optimization is performed in order to evaluate the compromises between plant efficiency and investment costs, as well as to investigate the influence of the parameters assumed as independent variables on these two fundamental aspects characterizing the system.

The total plant efficiency η_{tot} is assumed equal to that of the design day. For the economic aspect, the specific plant cost (ic_{tot}, total cost divided by the daily energy production) is taken as objective function. In addition, to compare the performance of different plant portions, the Calcium-Looping efficiency (η_{CaL}, defined as the daily electrical output divided by the net thermal power absorbed at the calciner) and the carbonator side efficiency (η_{CarbS}, computed as the ratio between the daily electrical output and the heat of reaction released in the carbonator) are defined. Finally, the independent variables of the problem, referred to their corresponding plant section, are summed up in Table 8.

The structure of the optimization process has been presented in Fig. 2. The separate optimization for the dimensioning of the charging section is performed on MATLAB by the fmincon function with a tolerance equal to 10^{-8}. The multi-objective optimization is instead performed with the gamultiobj function and the convergence was reached keeping the default tolerance, set to 10^{-4}. Finally, concerning the optimizations nested into the GA, the CaO flowrate is optimized with the bisection method, which is stopped when the relative error of the

Table 7
Thermal transfer coefficients.

Fluids	U [W/(m2K)]
CO2 - CO2	300
CO2 - He	300
He - He	700
He - air	300
CO2 - air	300

Table 8
Independent variables to optimize.

Power Block	Independent variables						
	C1IP	#C	$\beta_{C1/2/3/4}$	$\Delta T_{min,R}$	TIT	#T	$\beta_{T1/2/3}$
Carbonator Side	T_{CARB}	$T_{CaO,IN}$	$T_{CO2,IN}$	STIT	BIT	$\dot{m}_{CaO}$	HRCP/HTCW
Calciner and Solar Side	#IC	CPO					

solutions found in two consecutive steps is $\leq 10^{-5}$.

According to the number of individuals constituting the population, the process took at least 20 min, with a maximum of 2 h.

6. Results

From the multi-objective optimization emerges that the calciner side layout always reaches the same configuration. For this reason, it is separately exposed in the following subparagraph and successively the exposition of the results is more focused on the discharging process. Investment costs are expresses in $ at 2018.

6.1. Calciner side

The resulting calciner side layout is shown in Fig. 4. CO_2 intercooled compression schematized for sake of simplicity with a single compressor; however, five intercooling stages (the maximum set in the process) are the optimal value found by the algorithm. For this plant size, the only parameters that undergo variations between the configurations found in the Pareto curve are the components design size (and therefore their prices), that are dependent on the nominal flowrates of the charging process. Detailed data regarding operating conditions are reported in Appendix B.

6.2. Energy optimization results

The optimized layout of carbonator side and power block is shown in Fig. 5. The total plant efficiency is equal to 21.85%, while the specific investment cost is 185.6 $/MJ. The most important results for this configuration are summed up in Table 9; detailed data are reported in Appendix C.

The highest performances are obtained when the heat of reaction is recovered at the carbonator wall (HTCW). There are many aspects related to reheating and intercooling stages that influence the system efficiency. In fact, a higher number of compressors and turbines allows to reach better compression and expansion efficiency and at the same time, the pressure losses determined by intercoolers and reheaters introduce non-negligible penalties to the power block performance. As a result, three compressors and three turbines are found by the algorithm to be the optimal setting in order to achieve the maximum energy performance. Helium turbine inlet temperature arrives to 850 °C; first compressor and first turbine inlet pressures are 11.5 bar and 33.7 bar respectively. The three compressors show nearly identical values of pressure ratio (equal to 1.46) and the same is observed for the turbines (equal to 1.4).

Concerning the carbonator side, it is important to notice that the algorithm converges to a configuration in which the amount of CO_2 provided to the carbonation reaction is equal to the stoichiometric value. Since there is not a recirculating stream of CO_2 at the outlet of the reactor, it cannot be avoided to preheat the CaO with the $CaCO_3$ and the presence of a heat transfer fluid must be taken into account. At the end of the preheating process, CO_2 and CaO enter the carbonator at 714 °C and 761 °C respectively. Both carbonation temperature and storage turbine inlet temperature reach their maximum value. The heat recovery at the carbonator wall has two main consequences. First, the carbonator operation becomes more complex and its investment cost increase sensitively because of the presence of heat exchangers. Second, the carbonator side Heat Exchanger Network layout becomes simpler and the heat exchanger sizes are smaller, since it is only devoted to the reactants preheating.

Hot and cold composite curves are shown in Fig. 6a, while grand composite curve is presented in Fig. 6b. The fact that $CaCO_3$ and CaO unreacted are the only carbonator outflows (at high temperature) makes it impossible to avoid solid–solid thermal transfer in the heat recovery process. The presence of this phenomenon is coherently taken into account during the pinch analysis execution by properly modifying the minimum temperature difference achievable by this specific stream.

Investment cost of components and relative weight of plant sections costs are shown in Fig. 7. For the power block, turbomachinery are by far the most expensive components and the importance of the compression

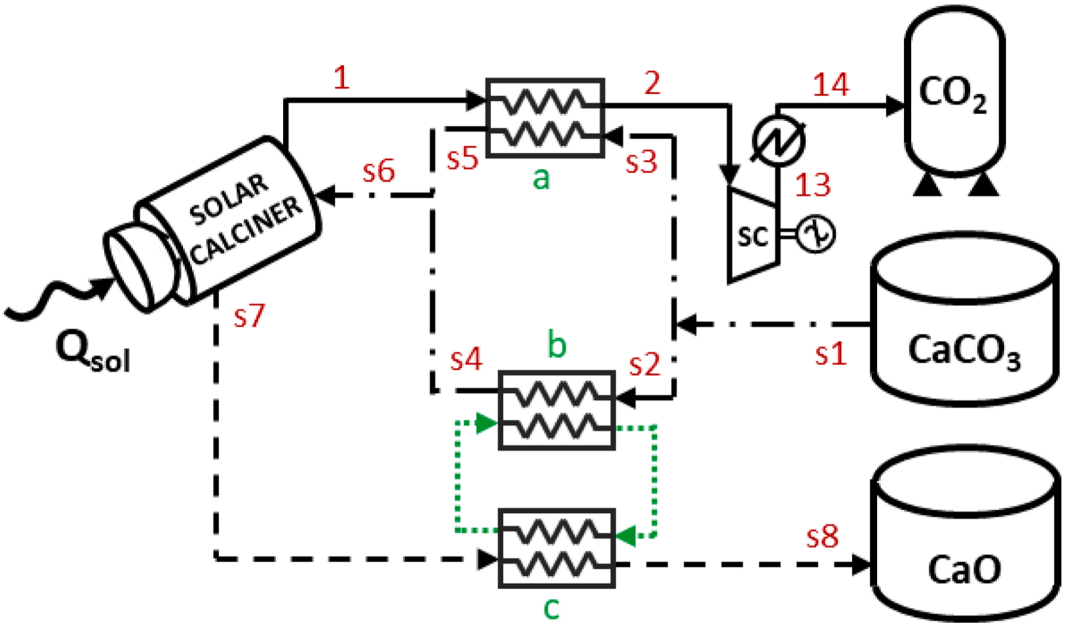

Fig. 4. Calciner side optimized layout.

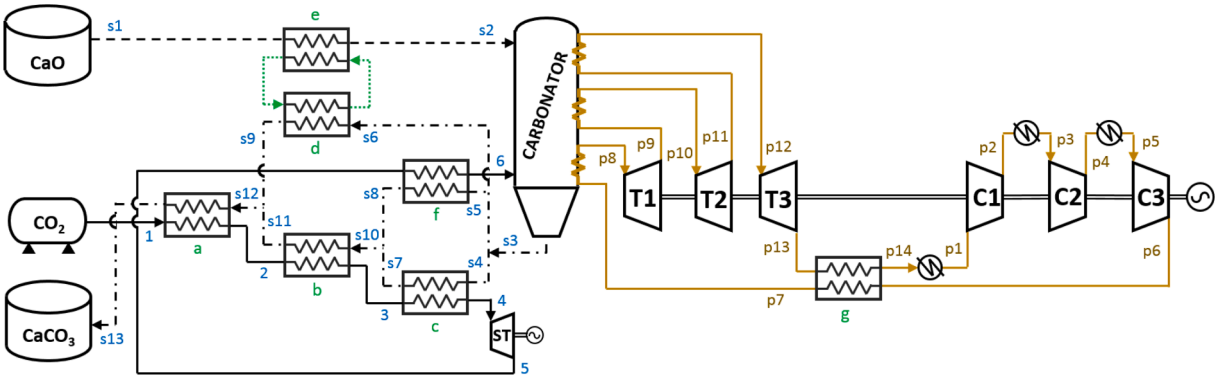

Fig. 5. Carbonator side and power block layout obtained from energy optimization.

Table 9
Design parameters for the energy-optimized layout.

η_{PB}	η_{CarbS}	η_{CaL}	η_{tot}
55.0%	53.0%	42.1%	21.9%
ic_{tot} [$/MJ]	IC_{tot} [M$]	$\Phi_{des,clc}$ [MW_t]	A_{helio} [m^2]
185.6	30.9	24.98	38′060

process is evident. As expected, heliostat field and central tower have the highest weight in relative terms to the total capital investment (36%). In addition, a very significant contribute is provided by the chemical reactors. It is interesting to notice that, despite a difference in size of more than five times, the carbonator reactor cost is nearly the double with respect to the solar calciner. This is due to the presence of a heat transfer at the carbonator wall. Compared to the cost of a reactor operating with supercritical CO_2, the cost is 150% higher (according to the methodology developed in the present work). In fact, the higher operating temperatures and, therefore, the lower difference between temperature of reaction and He temperature determine an increase of the surface area required for the heat exchange, which represents the highest contribute to the component cost.

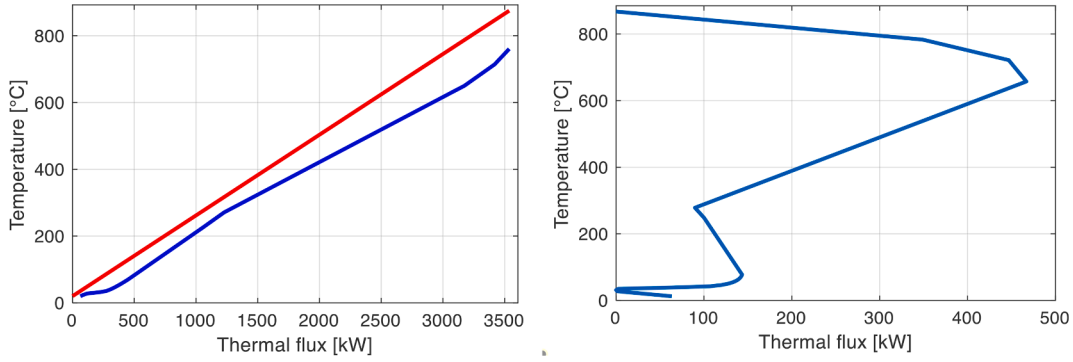

Fig. 6. Hot and cold composite curves (a, left) and grand composite curve (b, right) of carbonator side heat transfer process for energy optimization.

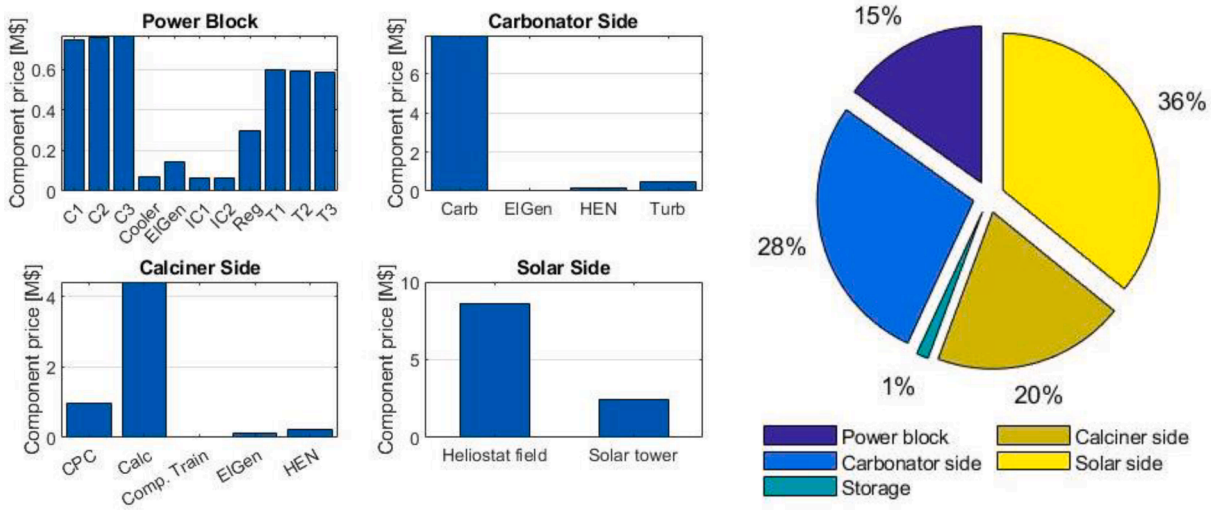

Fig. 7. Components investment costs (left, a) and percentage of total cost of plant sections (right, b).

6.3. Economic optimization results

The layout obtained from the economic optimization for the plant section devoted to the discharging process is shown in Fig. 8. The total efficiency is 18.1% and the specific investment cost reaches 169.2 $/MJ. Other benchmarks referred to this layout are reported in Table 10; detailed data are reported in Appendix D.

The algorithm converges to a configuration in which the power block is thermally fed through a heat recovery performed on the carbonator outflows (HRCP). Helium compression and expansion in the power block is performed with two turbines and three compressors. Turbines inlet temperature is slightly less than its maximum value (840 °C), while carbonation temperature is even in this case equal to 875 °C. First compressor and first turbine inlet pressures are 9.7 bar and 32.3 bar respectively. Turbomachinery pressure ratios tend to be slightly higher with respect to the results obtained from the energy optimization. Compressors pressure ratios are in the range between 1.46 and 1.59, while the values for turbines are 1.69 and 1.87.

Concerning the carbonator side, the HRCP configuration simplify the carbonator operation because of the use of the absence of heat transfer at the reactor wall, but it implies an increase in the Heat Exchanger Network layout complexity. In fact, there are two additional heat exchangers with respect to the energy-optimized layout. The amount of CO_2 provided to the carbonator is nine times the stoichiometric value, determining a significant flowrate recirculated. Temperatures of gaseous and solid streams entering the reactor are equal to 600 °C and 593 °C respectively. Finally, it is interesting to notice that the algorithm converges to a solution in which high-temperature heat of carbonator outflows is exclusively devoted to the power block thermal feeding, while the rest is left to the reactants preheating.

Hot and cold composite curves are shown in Fig. 9a, while grand composite curve is presented in Fig. 9b. It can be noticed that the algorithm converges to a solution with two pinch points (one around 160 °C and the other near 640 °C). This configuration is reached thanks to the significant amount of CO_2 provided in excess to the carbonator and recirculated in the discharging process. Consequently, the heat recovery size and complexity result to be higher with respect to the case previously analyzed.

Components investment costs and relative weight of the plant sections are reported in Fig. 10. Turbomachinery cost for the economic optimization is even higher with respect to the case of energy optimization. The power block cost constitutes the 21% of the total investment. The use of an adiabatic carbonator brings consistent economic benefits. The solar calciner does not undergo significant variations and nearly the same happens for the solar side. However, for the present configuration the relative weight of this last section reaches the 45% of the plant capital investment, while the storage contribute remains very low.

Table 10
Plant design parameters for the configuration obtained with economic optimization.

η_{PB}	η_{CarbS}	η_{CaL}	η_{tot}
53.3%	46.8%	36.1%	18.1%
ic_{tot} [$/MJ]	IC_{tot} [M$]	$\Phi_{des,clc}$ [MW_t]	A_{helio} [m^2]
169.1	26.1	24.68	42′519

6.4. Multi-objective optimization results

The Pareto curve obtained from the multi-objective optimization is shown in Fig. 11. The reason why it appears as a piecewise curve is because of the layout changes chosen by the algorithm itself. In the figure are reported, for the corresponding stretches, the values assumed by some parameters taken as independent variables. The solar side (SolS) is nearly always optimized in energy terms, except for the point on the far left of the graph. The number of compressor remain constant and equal to three in the entire length of the curve. Two turbines are present in case of power block thermal feeding executed with a Heat Recovery on Carbonator Products, while three are chosen when is performed a Heat Transfer on Carbonator Wall. The former configuration allows to reach the best results in economic terms and the latter layout makes possible to obtain the highest performances.

A significant variation is observed for the configuration with HTCW. The reason for this phenomenon is the strong influence of the inlet temperature of helium turbines in this specific configuration. This behavior emerges thanks to the strategy developed in the present work to adapt the cost function proposed in [48] (for a non-adiabatic carbonator operating with supercritical CO_2) to the present case study (in which helium is the power fluid). Both the fluids properties and the temperature differences are considered in order to apply this correction. As a consequence, keeping a high carbonation temperature and reducing

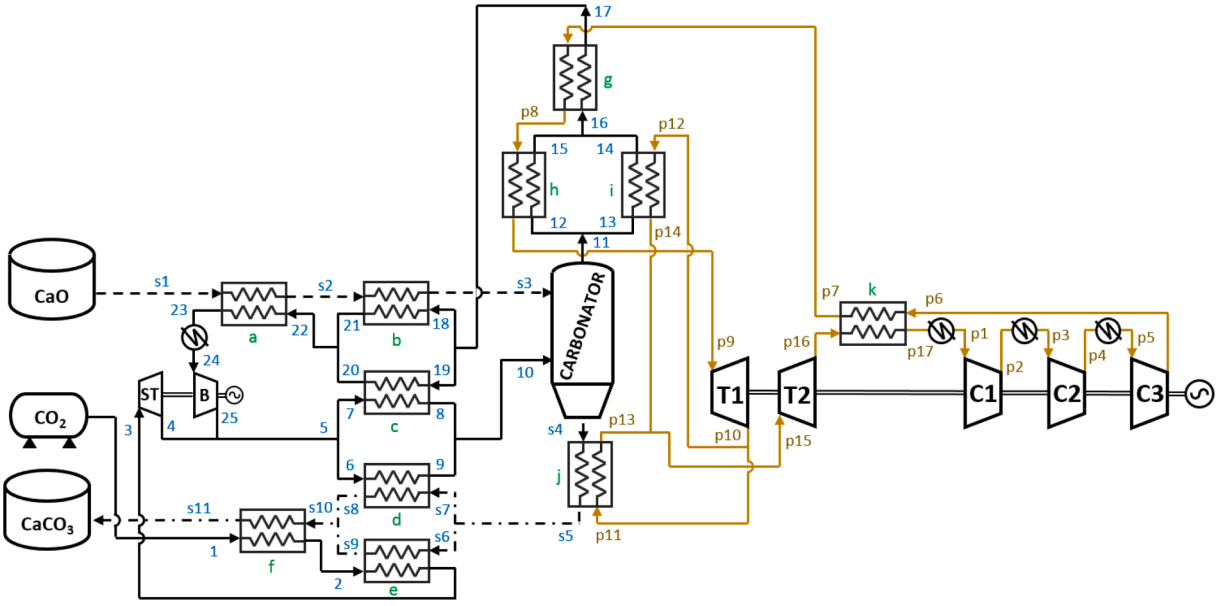

Fig. 8. Carbonator side and power block layout obtained from economic optimization.

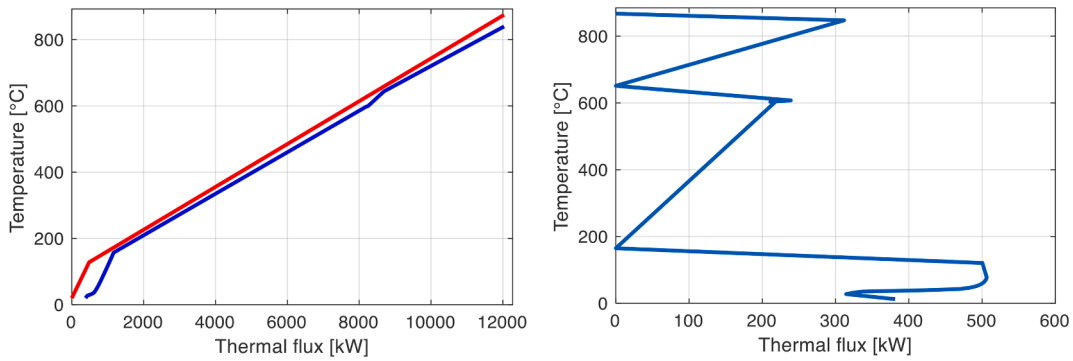

Fig. 9. Hot and cold composite curves (a, left) and grand composite curve (b, right) of carbonator side heat transfer process for economic optimization.

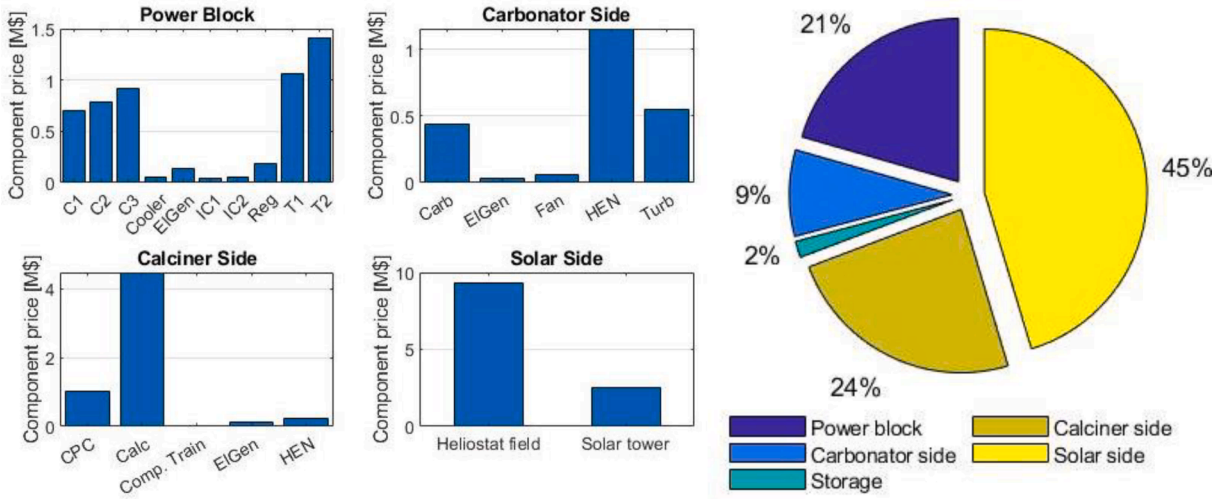

Fig. 10. Components investment costs (left, a) and percentage of total cost of plant sections (right, b).

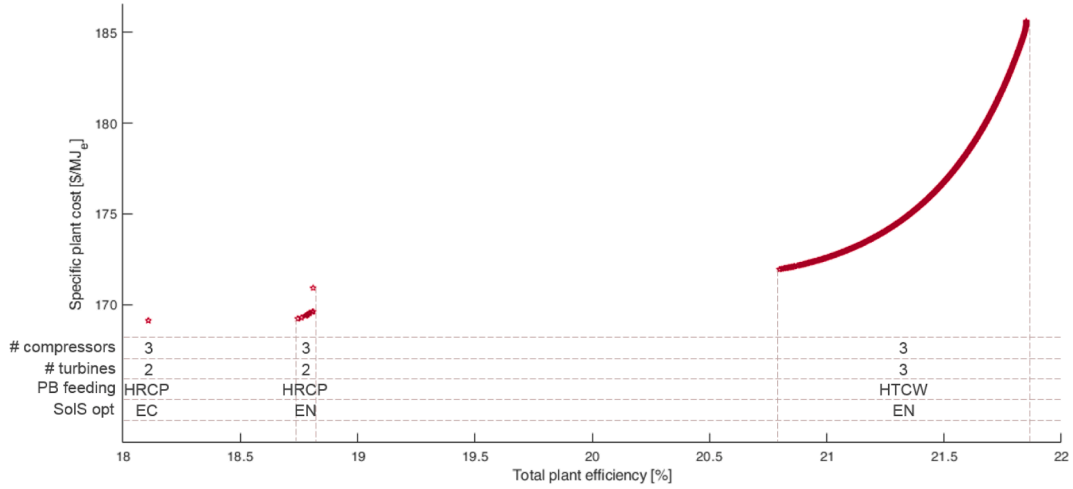

Fig. 11. Pareto curve for multi-objective optimization.

the helium maximum temperature allows to decrease the reactor investment cost (because of the higher temperature difference and, therefore, the lower heat transfer surface required) at the price of an efficiency penalty. For this reason, helium TIT changes from its maximum achievable (850 °C with efficiency equal to 21.85%) to 789 °C (with total efficiency 20.8%). The minimum temperature difference reached by the regenerator is another parameter that influences the system performance (although not so significantly as the one previously cited). Lower values allow a better heat recovery but, according to the methodology adopted, determine higher pressure losses. Considering these two conflicting aspects, the solution found by the algorithm show a minimum temperature difference equal to 8.2 °C (in case of maximum performance) that progressively rises up to 13.8 °C (for the economic optimization).

The trends assumed along the Pareto curve by the most representative independent variables (normalized for their corresponding variation ranges) is shown in Fig. 12. For the wide portion in which the algorithm converges to the HTCW configuration, it is possible to made the following considerations: i) reactants preheating is boosted by the absence of a power block thermal feeding performed on the carbonator outflows, therefore $T_{CaO,in}$, $T_{CO2,in}$, STIT and BIT achieve higher and constant values; ii) ΔT_{Reg} and TIT have opposite impacts on both plant performance and costs, however, ΔT_{Reg} variation is monotonous while the TIT trend changes when passing form HTCW to HRCP.

Finally, it is worth to discuss how the choice for the compromise between plant efficiency and costs is carried out by the algorithm. The cost of the charging plant section is always the most significant contribution to the total capital investment, therefore it could be expected that less performing power blocks require charging processes with higher sizes, introducing penalties in both energy and economic terms. However, results demonstrate the existence of configurations in which the costs increase related to the charging section is overcome by the price decrease occurring in the discharging process. This aspect is shown in Fig. 13, where the variation of the contribution to the specific plant cost of the two system sections is referred to the configuration obtained from the energy optimization.

7. Sensitivity analysis

The estimation of turbomachinery capital investment may be affected by uncertainties because of the absence of rigorous and validated cost functions in scientific literature. For this reason, a sensitivity analysis on the prices of these components is performed. The multi-objective optimization is carried out by new for any value assumed as percentage deviation, in order to evaluate not only the effects on the specific plant cost but also the possible changes occurring in the layouts resulting from the optimization process.

The sensitivity analysis results are shown in Fig. 14. Considering the Pareto curves for the cost deviations investigated (a), it is possible to notice that the differences in turbomachinery capital investment do not determine changes in the configurations to which the algorithm converges. In absolute terms, higher turbomachinery costs reduce the ic_{tot} difference encountered when the power block feeding passes from the case of HTCW to HRCP. In relative terms (b), the price variation has a higher impact on the HRCP configuration with respect to the HTCW; in this way, when the turbomachinery cost rises by 40%, ic_{tot} increases by

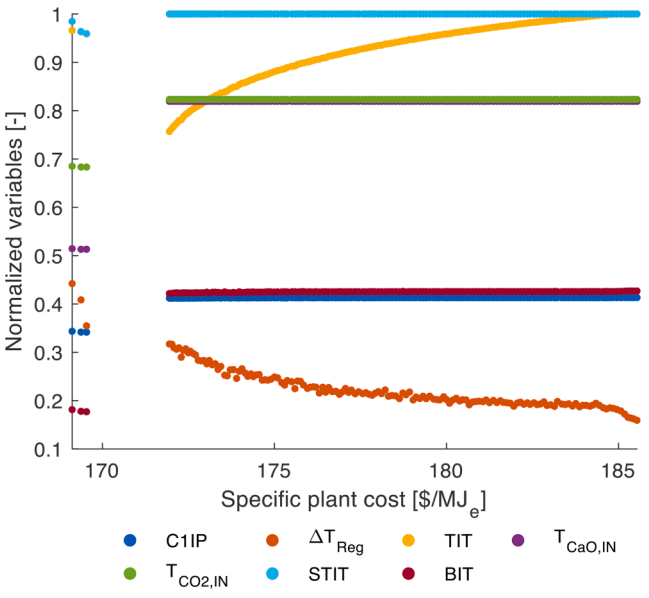

Fig. 12. Normalized variables trends along the Pareto curve.

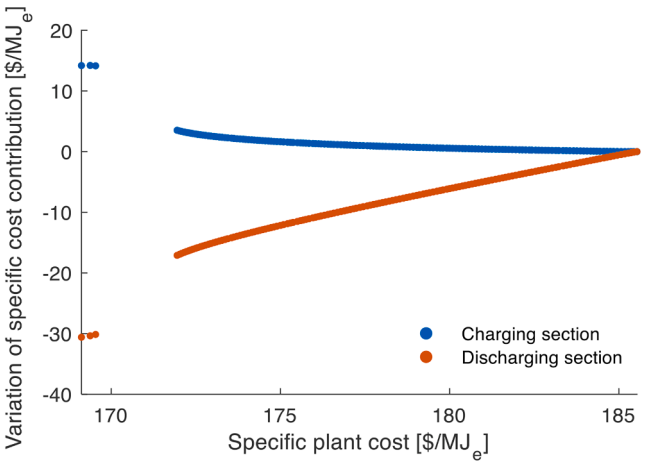

Fig. 13. Variation of the contribution to the specific plant cost of charging and discharging plant sections.

8% for the first case but by less than 6% for the second one.

8. Conclusions

The indirect integration of helium power cycles in a central tower Concentrated Solar Power plant with ThermoChemical Energy Storage based on Calcium-Looping is investigated in the present work. A suitable method must be used in order to optimize both the operating conditions and the heat transfer processes of the entire system. With this aim, the HEATSEP methodology is adopted, which includes pinch analysis, bisection and genetic algorithm as optimization methods, employed at different nesting levels. Various power block layouts are considered in form of superstructure and two different alternatives for the thermal feeding of the cycle are included (i.e. on the reactor wall or in the heat recovery process). A multi-objective optimization is performed in order to find the optimal results both in terms of system efficiency and investment costs and to investigate the influence of the independent variables on these two aspects. Finally, the sensitivity analysis on He turbomachinery cost is carried out to evaluate the effect of deviations in the estimation of their capital investment that may affect this technology.

As expected, highest energy performances (21.85%) are obtained when the heat is provided to the power cycle with a thermal transfer on the carbonator wall, whose price rises significantly because of the presence of heat exchangers. Lowest specific investment costs (169 $/MJ) are found in case of power cycle thermally fed with a Heat Recovery on Carbonator Products, which is a configuration that allows to use an adiabatic carbonator.

Helium expansion is performed with three turbines in the former case and two turbines in the latter, while the compression process is always performed with three compressors. Novel plant layouts are designed for the configurations obtained from energy and economic optimization and Heat Exchanger Network complexity of the discharging section results to be higher in the latter case. Performing the thermal feeding of the power block on the carbonator wall makes unnecessary the CO_2 recirculation and decreases the number of fluids involved in the heat recovery process. In addition, for this configuration the operating conditions of the reactants in the carbonator side reach constant values that optimize the heat recovery process.

Helium turbines inlet temperature and minimum temperature difference achievable in regenerator are found to be two of the most important parameters that influence the system performances and costs, able to move the optimality from the economic criterion to the energy criterion. Therefore, the choice of these parameters during the design stage of the plant must be carefully weighted.

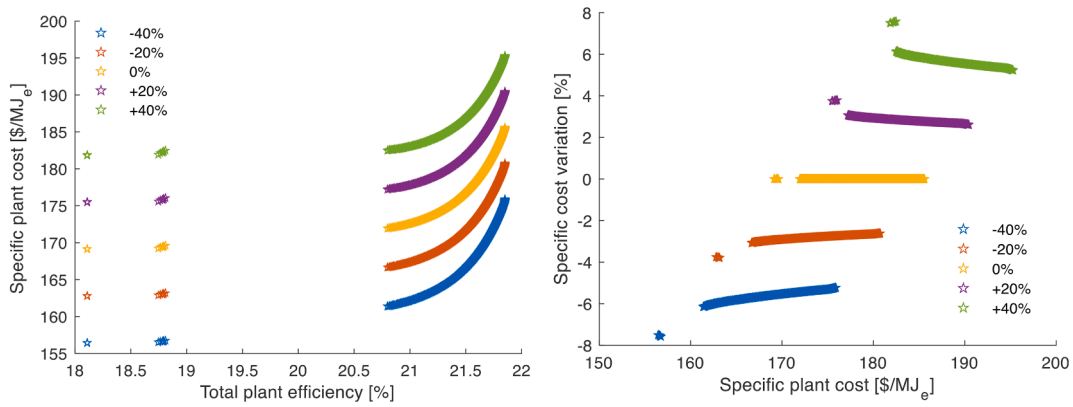

Fig. 14. Sensitivity analysis on turbomachinery cost. Pareto curves on the left (a) and relative variation on the right (b).

Finally, according to the sensitivity analysis performed, the specific plant investment cost varies from 5.5% to 8% when turbomachinery investment deviates by 40% from the predicted value. Results obtained demonstrate the interest in integrating efficient He thermal cycles operating at high temperatures in the Calcium-Looping, being competitive with other alternatives proposed in scientific literature.

CRediT authorship contribution statement

Umberto Tesio: Conceptualization, Methodology, Visualization, Writing – original draft, Writing – review & editing. **Elisa Guelpa:** Conceptualization, Methodology, Formal analysis. **Vittorio Verda:** Conceptualization, Methodology, Project administration, Funding acquisition.

Declaration of Competing Interest

The authors declare that they have no known competing financial interests or personal relationships that could have appeared to influence the work reported in this paper.

Acknowledgment

This work has been conducted within the European Project SOCRATCES (SOlar Calcium-looping integRAtion for Thermo-Chemical Energy Storage) GA 727348.

Appendix A. Fluidized Bed carbonator adaptation

For first, it is assumed (coherently to [53]) that the cost of a cooled Fluidized Bed reactor is determined for the 85% (α) by the heat exchangers. Therefore, taking the heat transfer surface (A) as scaling parameter, the reactor cost for helium as power fluid is adapted from the case of supercritical CO_2 with Eq. (2). Operating conditions and cost function (calculated with the same thermal power transferred on the reactor wall) for this last configuration are taken from [48].

$$IC_{He} = IC_{sCO_2} \cdot \left(\alpha \cdot \frac{A_{He}}{A_{sCO_2}} + (1-\alpha) \right) \tag{2}$$

The ratio of surface areas can be expressed with Eq. (3), where the heat exchanger area in case of helium is obtained taking into account the possibility of performing reheating stages.

$$\frac{A_{He}}{A_{SCO_2}} = \frac{\sum_i \left[\frac{\phi_{He,i}}{U_{He,i} \cdot \Delta T_{ml,He,i}} \right]}{\frac{\Phi_{sCO_2}}{U_{sCO_2} \cdot \Delta T_{ml,sCO_2}}} \tag{3}$$

In case of internal flow in a pipe, the overall heat transfer coefficient (U) can be approximated with Eq. (4), where h_{int} is the convective heat transfer coefficient corresponding to the power fluid, while h_{ext} is referred to the external mass flow. Assuming a fully developed turbulent flow, the former parameter is computed with the Dittus-Boelter correlation (considering the same hydraulic diameter) and the latter one is taken from [54]. The helium velocity is imposed, while the sCO_2 velocity is obtained from an energy balance (Eq. (5)); for both the cases, the assumption of turbulent flow must be verified.

$$U \cong \left[\frac{1}{h_{int}} + \frac{1}{h_{ext}} \right]^{-1} \tag{4}$$

$$\frac{v_{sCO_2}}{v_{He}} = \frac{\rho_{He} \cdot c_{p\,He} \cdot \Delta T_{He}}{\rho_{sCO_2} \cdot c_{p\,sCO_2} \cdot \Delta T_{sCO_2}} \tag{5}$$

Finally, the logarithmic mean temperature difference is calculated with inlet/outlet temperatures of power fluid and the reactor operating temperature.

Appendix B. Calciner side optimization results

	s1	s2	s3	s4	s5	s6	s7	s8	1	2	3	4	5	6	7	8	9	10	11	12	13	14
P [bar]	–	–	–	–	–	–	–	–	1	1	2.1	2	4.2	4.2	8.7	8.6	17.9	17.7	36.8	36.5	75.8	75
T [°C]	20	20	20	841.2	878.9	853.2	950	50	950	35	109.5	35	101.6	35	100.7	35	100.8	35	101.3	35	101.6	35

	Flowrate split
s2	68.0%
s3	32.0%

Appendix C. Energy optimization results

	P [bar]	T [°C]	$\dot{m}$[kg/s]		P [bar]	T [°C]	$\dot{m}$[kg/s]		P [bar]	T [°C]	$\dot{m}$[kg/s]
s1	–	20	2.83	s12	–	85.8	3.94	p4	24.0	90.9	1.75
s2	–	761	2.83	s13	–	35	3.94	p5	23.6	35	1.75
s3	–	875	3.94	1	75	20	1.11	p6	34.6	91.1	1.75
s4	–	875	0.83	2	74.8	45.8	1.11	p7	34.4	712.1	1.75
s5	–	875	0.94	3	74.5	271	1.11	p8	33.7	850	1.75
s6	–	875	2.17	4	74.3	650	1.11	p9	24.1	718.4	1.75
s7	–	301	0.83	5	1.11	271	1.11	p10	23.6	850	1.75
s8	–	301	0.94	6	1.04	714	1.11	p11	16.9	718.9	1.75
s9	–	50	2.17	p1	11.5	35	1.75	p12	16.6	850	1.75
s10	–	301	1.77	p2	16.7	90.6	1.75	p13	11.9	720.4	1.75
s11	–	130	1.77	p3	16.4	35	1.75	p14	11.6	99.4	1.75

Turbomachinery design powers				Carbonator side and power block HEXs design powers			
$\dot{W}_{T1}[kW]$	1195	$\dot{W}_{C1}[kW]$	505	a [kW_t]	209	e [kW_t]	1885
$\dot{W}_{T2}[kW]$	1191	$\dot{W}_{C2}[kW]$	508	b [kW_t]	317	f [kW_t]	576
$\dot{W}_{T3}[kW]$	1177	$\dot{W}_{C3}[kW]$	510	c [kW_t]	496	g [kW_t]	5641
$\dot{W}_{ST}[kW]$	474			d [kW_t]	1885		
Daily auxiliaries consumptions				Calciner side HEXs design powers			
$E_{conv}[MJ_e]$	5855	$E_{hr}[MJ_e]$	349	a [kW_t]	4481	b [kW_t]	9119
Calciner side design flowrates				c [kW_t]	9119		
$CaCO_3 + CaO_{un}$ [kg/s]		15.5					
CaO [kg/s]	11.1	CO_2 [kg/s]	4.4				

Appendix D. Economic optimization results

	P [bar]	T [°C]	$\dot{m}$[kg/s]		P [bar]	T [°C]	$\dot{m}$[kg/s]		P [bar]	T [°C]	$\dot{m}$[kg/s]
s1	–	20	3.1	8	1.04	600	3.1	p1	9.7	35	1.64
s2	–	157	3.1	9	1.04	600	7.7	p2	14.2	91	1.64
s3	–	593	3.1	10	1.04	600	10.8	p3	14.0	35	1.64
s4	–	875	4.3	11	1.04	875	9.6	p4	21.1	97	1.64
s5	–	659	4.3	12	1.04	875	6.8	p5	20.8	35	1.64
s6	–	659	1.3	13	1.04	875	2.8	p6	33.0	105	1.64
s7	–	659	3.0	14	1.03	659	2.8	p7	32.9	596	1.64
s8	–	172	3.0	15	1.03	659	6.8	p8	32.6	644	1.64
s9	–	172	1.3	16	1.03	659	9.6	p9	32.3	840	1.64
s10	–	172	4.3	17	1.02	622	9.6	p10	19.1	644	1.64
s11	–	59	4.3	18	1.02	622	2.3	p11	19.1	644	0.95
1	75	20	1.2	19	1.02	622	7.3	p12	19.1	644	0.69
2	74.7	157	1.2	20	1.01	172	7.3	p13	18.8	840	0.95
3	74.3	644	1.2	21	1.01	172	2.3	p14	18.8	840	0.69
4	1.11	267	1.2	22	1.01	172	9.6	p15	18.8	840	1.64
5	1.11	157	10.8	23	1	138	9.6	p16	10	609	1.64
6	1.11	157	7.7	24	1	127	9.6	p17	9.9	118	1.64
7	1.11	157	3.1	25	1.11	143	9.6				

Turbomachinery design powers				Carbonator side and power block HEXs design powers			
$\dot{W}_{T1}[kW]$	1672	$\dot{W}_{C1}[kW]$	476	a [kW_t]	369	g [kW_t]	409
$\dot{W}_{T2}[kW]$	1964	$\dot{W}_{C2}[kW]$	526	b [kW_t]	1178	h [kW_t]	1673
$\dot{W}_{ST}[kW]$	508	$\dot{W}_{C3}[kW]$	594	c [kW_t]	3776	i [kW_t]	706
		$\dot{W}_{B}[kW]$	135	d [kW_t]	1494	j [kW_t]	966
Daily auxiliaries consumptions				e [kW_t]	682	k [kW_t]	4188
$E_{conv}[MJ_e]$	6319	$E_{hr}[MJ_e]$	376	f [kW_t]	413		
Calciner side design flowrates				**Calciner side HEXs design powers**			
$CaCO_3 + CaO_{un}$ [kg/s]		15.9		a [kW_t]	4596	b [kW_t]	9354
CaO [kg/s]	11.4	CO_2 [kg/s]	4.5	c [kW_t]	9354		

References

[1] International Renewable Energy Agency, "Renewable Power Generation Costs in 2017," 2018.

[2] K. Lovegrove, G. James, D. Leitch, A. Milczarek, A. Ngo, J. Rutovitz, M. Watt and J. Wyder, "Comparison of dispatchable renewable electricity options - Technologies for an orderly transition," 2018.

[3] Pelay U, Luo L, Fan Y, Stitou D, Rood M. Thermal energy storage systems for concentrated solar power plants. Renew Sustain Energy Rev 2017;79:82–100.

[4] González-Roubaud E, Pérez-Osorio D, Prieto C. Review of commercial thermal energy storage in concentrated solar power plants: steam vs. molten salts. Renew Sustain Energy Rev 2017;80:133–48.

[5] Bayon A, Bader R, Jafarian M, Fedunik-Hofman L, Sun Y, Hinkley J, et al. Techno-economic assessment of solid–gas thermochemical energy storage systems for solar thermal power applications. Energy 2018;149:473–84.

[6] K. Kyaw, M. Hitoki, H. Masanobu, "Applicability Of Carbonation/Decarbonation Reactions For Storing Thermal Energy From Nuclear Reactors," *Proceedings of the 3rd JAERI symposium on HTGR technologies,* 1996.

[7] Ortiz C, Valverde J, Chacartegui R, Perez-Maqueda L. Carbonation of limestone derived CaO for thermochemical energy storage: from kinetics to process integration in concentrating solar plants. ACS Sustain Chem Eng 2018;6:6404–17.

[8] Perejón A, Romeo LM, Lara Y, Lisbona P, Martínez A, Valverde JM. The Calcium-looping technology for CO2 capture: on the important roles of energy integration and sorbent behavior. Appl Energy 2016;162:787–807.

[9] Sanchez-Jimenez PE, Valverde JM, Perez-Maqueda LA. Multicyclic conversion of limestone at Ca-looping conditions: the role of solid-sate diffusion controlled carbonation. Fuel 2014;127:131–40.

[10] Sánchez Jiménez PE, Perejón A, Benítez Guerrero M, Valverde JM, Ortiz C, Pérez Maqueda LA. High-performance and low-cost macroporous calcium oxide based materials for thermochemical energy storage in concentrated solar power plants. Appl Energy 2019;235:543–52.

[11] Benitez-Guerrero M, Valverde JM, Sanchez-Jimenez PE, Perejon A, Perez-Maqueda LA. Multicycle activity of natural CaCO3 minerals for thermochemical energy storage in concentrated solar power plants. Sol Energy 2017;153:188–99.

[12] Algieri A, Morrone P. Comparative energetic analysis of high-temperature subcritical and transcritical organic rankine cycle (ORC). A biomass application in the Sibari district. Appl Therm Eng 2012;36:236–44.

[13] Cheang V, Hedderwick R, McGregor C. Benchmarking supercritical carbon dioxide cycles against steam Rankine cycles for concentrated solar power. Sol Energy 2015;113:199–211.

[14] Javanshir A, Sarunac N, Razzaghpanah Z. Thermodynamic analysis of simple and regenerative Brayton cycles for the concentrated solar power applications. Energy Convers Manage 2018;163.

[15] Yang J, Yang Z, Duan Y. Novel design optimization of concentrated solar power plant with S-CO2 Brayton cycle based on annual off-design performance. Appl Therm Eng 2021;192:116924.

[16] Ma Y, Morosuk T, Luo J, Liu M, Liu J. Superstructure design and optimization on supercritical carbon dioxide cycle for application in concentrated solar power plant. Energy Convers Manage 2020;206:112290.

[17] Thanganadar D, Fornarelli F, Camporeale S, Asfand F, Gillard J, Patchigolla K. Thermo-economic analysis, optimisation and systematic integration of supercritical carbon dioxide cycle with sensible heat thermal energy storage for CSP application. Energy 2022;238:121755.

[18] Bahari M, Ahmadi A, Dashti R. Exergo-economic analysis and optimization of a combined solar collector with steam and Organic Rankine Cycle using particle swarm optimization (PSO) algorithm. Clean Eng Technol 2021;4:100221.

[19] Orsini RM, Brodrick PG, Brandt AR, Durlofsky LJ. Computational optimization of solar thermal generation with energy storage. Sustain Energy Technol Assess 2021;47.

[20] Liang Y, Chen J, Yang Z, Chen J, Luo X, Chen Y. Economic-environmental evaluation and multi-objective optimization of supercritical CO2 based-central tower concentrated solar power system with thermal storage. Energy Convers Manage 2021;238.

[21] Liang Y, Chen J, Luo X, Chen J, Yang Z, Chen Y. Simultaneous optimization of combined supercritical CO2 Brayton cycle and organic Rankine cycle integrated with concentrated solar power system. J Clean Product 2020;266.

[22] Chacartegui R, Alovisio A, Ortiz C, Valverde J, Verda V, Becerra J. Thermochemical energy storage of concentrated solar power by integration of the calcium looping process and a CO2 power cycle. Appl Energy Jul. 2016;173:589–605.

[23] Alovisio A, Chacartegui R, Ortiz C, Valverde J, Verda V. Optimizing the CSP-calcium looping integration for thermochemical energy storage. Energy Convers Manage Mar. 2017;136:85–98.

[24] Kemp I. Pinch analysis and process integration. Butterworth-Heinemann; 2007.

[25] Ortiz C, Romano M, Valverde J, Binotti M, Chacartegui R. Process integration of calcium-looping thermochemical energy storage system in concentrating solar power plants. Energy 2018;155:535–51.

[26] Ortiz C, Chacartegui R, Valverde J, Alovisio A, Becerra J. Power cycles integration in concentrated solar power plants with energy storage based on calcium looping. Energy Convers Manage 2017;149:815–29.

[27] Ortiz C, Valverde J, Chacartegui R, Perez-Maqueda L, Giménez P. The calcium-looping (CaCO3/CaO) process for thermochemical energy storage in concentrating solar power plants. Renew Sustain Energy Rev 2019;113.

[28] Tesio U, Guelpa E, Verda V. Integration of thermochemical energy storage in concentrated solar power. Part 1: Energy and economic analysis/optimization. Energy Convers Manage: X 2020;6:100039.

[29] Tesio U, Guelpa E, Verda V. Integration of thermochemical energy storage in concentrated solar power. Part 2: comprehensive optimization of supercritical CO2 power block. Energy Convers Manage X 2020;6:100038.

[30] Toffolo A, Lazzaretto A, Morandin M. The HEATSEP method for the synthesis of thermal systems: an application to the S-Graz cycle. Energy 2010;35:976–81.

[31] Alali AE, Al-Shboul KF. Performance analysis of the closed Brayton power cycle in a small-scale pebble bed gas cooled reactor using different working fluids. Ann Nucl Energy 2018;121:316–23.

[32] No Hee Cheon, Kim Ji Hwan, Kim Hyeun Min. A review of helium gas turbine technology for high-temperature gas-cooled reactors. Nucl Eng Technol 2007.

[33] McDonald CF. Helium turbomachinery operating experience from gas turbine power plants and test facilities. Appl Therm Eng 2012;44:108–42.

[34] K. Kusterer, R. Braun, N. Moritz , T. Sugimoto, K. Tanimura and D. Bohn, "Comparative Study Of Solar Thermal Brayton Cycles Operated With Helium Or Argon," *Proceedings of the ASME Turbo Expo 2013: Turbine Technical Conference and Exposition. Volume 4: Ceramics; Concentrating Solar Power Plants; Controls, Diagnostics and Instrumentation; Education; Electric Power; Fans and Blowers.,* 2013.

[35] Zare V, Hasanzadeh M. Energy and exergy analysis of a closed brayton cycle-based combined cycle for solar power tower plants. Energy Convers Manage 2016;128:227–37.

[36] Olumayegun O, Wang M, Kelsall G. Closed-cycle gas turbine for power generation: a state-of-the-art review. Fuel 2016;180:694–717.

[37] Dostál V, Hejzlar P, Driscoll MJ. The supercritical carbon dioxide power cycle: comparison to other advanced power cycles. Nucl Technol 2006;154:283–301.

[38] Zhao H, Peterson PF. Multiple reheat helium Brayton cycles for sodium cooled fast reactors. Nucl Eng Des 2008;238:1535–46.

[39] C. Wang, R. Ballinger, P. Stahle, E. Demetri and M. Koronowski, "Design of a power conversion system for an indirect cycle, helium cooled pebble bed reactor system," International Atomic Energy Agency, 2002.

[40] C. F. McDonald, "Helium and Combustion Gas Turbine Power Conversion Systems Comparison," *Proceedings of the ASME 1995 International Gas Turbine and Aeroengine Congress and Exposition. Volume 3: Coal, Biomass and Alternative Fuels; Combustion and Fuels; Oil and Gas Applications; Cycle Innovations.,* 1995.

[41] Lazzaretto A, Toffolo A. A method to separate the problem of heat transfer interactions in the synthesis of thermal systems. Energy 2008;33:163–70.

[42] Qiu Y, He Y-L, Du B-C. A comprehensive model for analysis of real-time optical performance of a solar power tower with a multi-tube cavity receiver. Appl Energy 2017;185:589–603.

[43] Meier A, Gremaud N, Steinfeld A. Economic evaluation of the industrial solar production of lime. Energy Convers Manage 2005;46:905–26.

[44] K. W. Battleson, "Solar power tower design guide: solar thermal central receiver power systems. A source of electricity and/or process heat," Sandia National Labs, 1981.

[45] Moumin G, Ryssel M, Zhao L, Markewitz P, Sattler C, Robinius M, et al. CO2 emission reduction in the cement industry by using a solar calciner. Renewable Energy 2020;145:1578–96.

[46] De Lena E, Spinelli M, Gatti M, Scaccabarozzi R, Campanari S, Consonni S, et al. Techno-economic analysis of calcium looping processes for low CO2 emission cement plants. Int J Greenhouse Gas Control 2019;82:244–60.
[47] M. Jonemann, "Advanced Thermal Storage System with Novel Molten Salt," National Renewable Energy Laboratory, 2013.
[48] Michalski S, Hanak D, Manovic V. Techno-economic feasibility assessment of calcium looping combustion using commercial technology appraisal tools. J Cleaner Prod 2019;219:p. 540e551.
[49] Zare V, Mahmoudi S, Yari M. An exergoeconomic investigation of waste heat recovery from the Gas Turbine-Modular Helium Reactor (GT-MHR) employing an ammonia–water power/cooling cycle. Energy 2013;61:397–409.
[50] Albrecht K, Ho C. Design and operating considerations for a shell-and-plate, moving packedbed, particle-to-sCO2 heat exchanger. Sol Energy 2019;15:331–40.
[51] Benjelloun M, Doulgeris G, Singh R. A method for techno-economic analysis of supercritical carbon dioxide cycles for new generation nuclear power plants. Proc Inst Mech Eng Part A J Power Energy 2012;226:372–83.
[52] S. E. Mink, S. E. Gedal, D. M. Weber and A. Dantuluri, "High-Temperature Nuclear Power Cycle Using Either Helium or s-CO2," 2016.
[53] Romano MC, Spinelli M, Campanari S, Consonni S, Cinti G, Marchi M, et al. The Calcium looping process for low CO2 emission cement and power. Energy Procedia 2013;37:7091–9.
[54] Spinelli M, Martínez I, Romano M. One-dimensional model of entrained-flow carbonator for CO2 capture in. Chem Eng Sci 2018:100–14.